

# Carrier Transport Model for Lateral $p$ - $i$ - $n$ Photodiodes at High-Frequency Operation

K. Konno, O. Matsushima, K. Hara, G. Suzuki, D. Navarro, and M. Miura-Mattausch

*Graduate School of Advanced Sciences of Matter,*

*Hiroshima University, Higashi-Hiroshima 739-8530, Japan*

Phone: +81-82-424-7637, FAX: +81-82-424-7638, E-mail: kohkichi@hiroshima-u.ac.jp

## 1. Introduction

The continuous shrinking of device dimension is associated with the interconnection bottleneck[1]; that is, interconnection propagation delay overwhelms transistor gate delay. This impedes fast switching operation of circuits. Under such a situation, optical interconnection becomes an attractive option, which involves light emitting devices, optical waveguide and photodetectors[1]. In order to design optoelectronic integrated circuits (OEIC), models describing the electronic and optical characteristics of optoelectronic devices for circuit simulation become a necessity. However, few works related to modeling of optoelectronic devices have been done so far.

We focus on photodiode as an optoelectronic device. Though the vertical type has been studied theoretically by some authors[2], theoretical work on the lateral photodiode is still lacking. The high frequency characteristics of vertical  $p$ - $i$ - $n$  photodiodes are known to be limited by the absorption length of the incident light. This is due to the trade-off between carrier transit distance and light absorption depth. However, the lateral  $p$ - $i$ - $n$  photodiode[3] is free from such limitation because the carrier path and light direction are different. This enables both high responsivity and high speed device operation. Furthermore, it realizes fabrication of silicon monolithic photodetectors since the technology is compatible to VLSI processes.

In this paper, we report a formulation of carrier transport in a lateral  $p$ - $i$ - $n$  photodiode. Computational accuracy of the model is comparable with the 2-dimensional device simulator MEDICI[4] yet the computational time is greatly reduced. Since the model equations are solved in the frequency domain, it is applicable for harmonic balance simulation[5].

## 2. Description of Carrier Transport

We consider a simplified structure of a lateral  $p$ - $i$ - $n$  photodiode shown in Fig. 1. The following assumptions are adopted in formulating the device equations: (1) homogeneous irradiation on the  $i$ -region, (2) constant electric field  $\mathbf{E} = (E_0^x, 0)$  in the  $i$ -region, (3) deep  $n^+$ - and  $p^+$ -region compared to the incident light penetration depth, and (4) negligible change of electric field  $E_0^x$  due to the incident pulse. (See e.g. Ref. [6] for high illumination.) These assumptions allow us to focus only on the  $i$ -region. Furthermore, the second assumption implies that carriers move along the  $x$ -direction.

A non-stationary description of carrier transport in the  $i$ -region is obtained using Fourier expansion. We expand time dependent variables as  $f(x, y, t) = \sum_{\omega_i} f_{\omega_i}(x, y) e^{-i\omega_i t}$ , where  $f$  denotes all the different de-

pendent variables, e.g. carrier number density, current density, photon flux, etc. By solving consistently the continuity equation and the current-density equation under the drift approximation with the boundary conditions,  $n_{\omega_i}(0, y) = 0$  and  $p_{\omega_i}(L, y) = 0$ , we obtain the solution for photocurrent as

$$I = q\mu E_0^x W \sum_{\omega_i} \left[ \frac{i}{\omega_i} \left\{ 1 - \exp \left( -i \frac{\omega_i}{\mu E_0^x} L \right) \right\} \right] \phi_{\omega_i} e^{-i\omega_i t},$$

where  $q$  is the elementary charge,  $\mu$  is the carrier mobility,  $\phi_{\omega_i}$  is the  $\omega_i$ -component of photon flux  $\phi(t)$ ,  $L$  is the  $i$ -region length along  $x$ -direction, and  $W$  is the width of the photodiode.

## 3. Modeling Results and Discussion

The real part of  $I_{\omega_i}$ , normalized by the low frequency value as a function of  $\omega_i$ , exhibits the frequency response of the photodiode. Cut-off frequency  $f_T$  is derived as the value of  $\text{Re}[I_{\omega_i}]$  at  $-3\text{dB}$ . Using the developed model, two methods for enhancing the frequency response are recognized. One method is by increasing the applied bias, which increases  $f_T$  as depicted by the horizontal line in Fig. 2. The next is by reducing the  $i$ -region length  $L$ . Figure 3 shows increasing  $f_T$  as  $L$  is reduced for two different applied biases. Steep increase in  $f_T$  is observed for  $L$  below  $1\mu\text{m}$ .

Next, we validate the accuracy of our model with measured transient photocurrent response of a fabricated Si lateral  $p$ - $i$ - $n$  photodiode. The device structure is shown in Fig. 4 with  $i$ -region length  $L=2\mu\text{m}$  and applied bias  $V_{pn}=7\text{V}$ . For our calculation, we adopt the spectral method[7] using the Fast Fourier Transform (FFT) in obtaining the time-domain model response. The model correctly reproduces measured photocurrent response for a Gaussian light pulse with  $\sim 60\text{ps}$  FWHM as shown in Fig. 5a. The difference in the end region can be attributed to carriers generated in the  $p^+$  and/or  $n^+$  region due to diffraction along the perimeter of the Al opening.

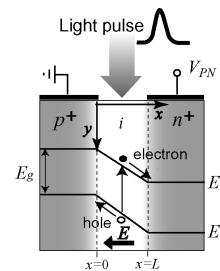


Figure 1: Structure of a lateral  $p$ - $i$ - $n$  photodiode.

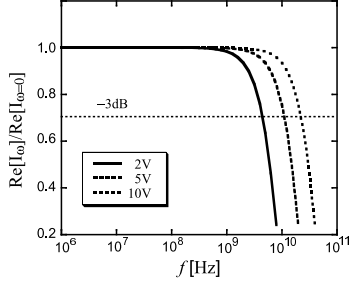


Figure 2: Cut-off frequency  $f_T$  increases as the applied bias is increased.  $f_T$  is approximated as the value of the  $\text{Re}[I_{\omega_i}]$  at  $-3\text{dB}$ .

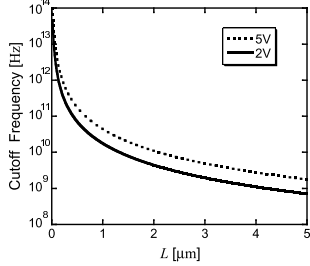


Figure 3: Cut-off frequency as a function of the  $i$ -region length  $L$ .

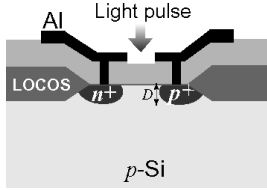


Figure 4: Fabricated lateral  $p$ - $i$ - $n$  photodiode.  $D$  ( $\sim 1\mu\text{m}$ ) depicts the diffusion depth. Doping density of substrate,  $n^+$  and  $p^+$  is  $\sim 10^{15}\text{cm}^{-3}$ ,  $10^{20}\text{cm}^{-3}$  and  $10^{20}\text{cm}^{-3}$ , respectively.

Computational accuracy of the model as compared with MEDICI is shown in Fig. 5b.

We demonstrate the photodiode frequency response using the model in Fig. 6. For a sinusoidal input of 1GHz, the photocurrent response exhibits no transit delay as shown in Fig. 6a. At 10GHz, which is in the cut-off region, the photocurrent shows phase shift and reduced amplitude as shown in Fig. 6b. Both are due to the fact that carriers can no longer respond to very fast switching input.

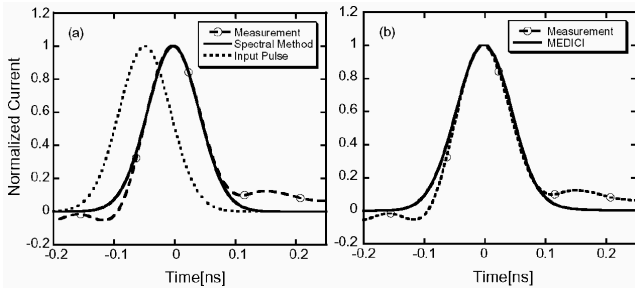


Figure 5: Normalized photocurrent calculated using the spectral method. (a) Calculated transit delay agrees with experimental result. (b) Computational accuracy is comparable with the two-dimensional device simulator MEDICI.

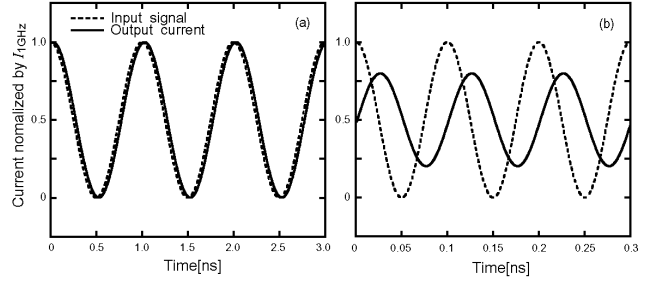


Figure 6: Photodiode response for (a) 1GHz and (b) 10GHz input. No photocurrent delay is observed at low switching frequency. At higher switching, photocurrent exhibits delay and reduced amplitude. Current is normalized with respect to the photocurrent at 1GHz.

Table 1: Features of the developed model as compared with MEDICI.

	Developed Model	MEDICI
Domain	Frequency	Time
Method	Analytical solution + FFT	Finite difference
Calculation time	$\lesssim 1\text{sec}$	$\sim 1\text{min}$
Compatibility with circuit simulation engine	· Harmonic Balance Simulator · SPICE via FFT	—

## 4. Conclusion

We have developed an analytical model for the carrier transport in lateral  $p$ - $i$ - $n$  photodiode. The frequency response of the photodiode is enhanced by shorter  $i$  region and higher applied bias. The model achieves excellent reproduction of measured photocurrent down to  $\sim 60\text{ps}$ . Furthermore, the developed model is appropriate for circuit simulation of OEICs. Table 1 summarizes other features of the developed model.

## References

- [1] L. C. Kimerling, Appl. Surf. Sci. **159-160**, 8 (2000)
- [2] G. Torrese et al., Microw. Opt. Tech. Lett. **31**, 329 (2001); K. Konno et al., Submitted to J. Appl. Phys. (2004); and references therein.
- [3] H. Hanafusa et al., J. Vac. Sci. Tech. **B11**, 1172 (1993); Y. S. He et al., Electron. Lett. **30**, 1887 (1994); M. Ghioni et al., IEEE Trans. Electron Device **43**, 1054 (1996); L. C. Schow et al., IEEE J. Quan. Electron. **35**, 1478 (1999); M. Yang et al., IEEE Electron Device Lett. **23**, 395 (2002)
- [4] MEDICI User's Manual, Synopsys (2002)
- [5] See e.g. K. S. Kundert, A. Sangiovanni-Vincentelli, IEEE Trans. CAD-5, 521 (1986)
- [6] O. Matsushima et al., Semicond. Sci. Tech. **19**, S185(2004); K. Konno et al., Appl. Phys. Lett. **84**, 1398(2004)
- [7] See e.g. B. Mercier, *An Introduction to the Numerical Analysis of Spectral Methods* (Springer-Verlag, Berlin, 1989)